Carbon 189 (2022) 37–45

Contents lists available at ScienceDirect

Carbon

journal homepage: www.elsevier.com/locate/carbon

Insights into fullerene polymerization under the high pressure: The role of endohedral Sc dimer

S.V. Erohin [a, b], V.D. Churkin [a, c], N.G. Vnukova [d, e], M.A. Visotin [d, e], E.A. Kovaleva [e, f], V.V. Zhukov [a, b, c], L.Yu. Antipina [g], Ye.V. Tomashevich [h], Yu.L. Mikhlin [h], M.Yu. Popov [a, b, c, **], G.N. Churilov [d, e], P.B. Sorokin [a, b, c, *], A.S. Fedorov [d, e, ***]

[a] Technological Institute for Superhard and Novel Carbon Materials, 7a Tsentralnaya Street, Troitsk, Moscow, Russian Federation
[b] National University of Science and Technology MISiS, 119049, Leninskiy prospect 4, Moscow, Russian Federation
[c] Moscow Institute of Physics and Technology, Institute lane 9, Dolgoprudniy, Moscow region, Russian Federation
[d] Institute of Engineering Physics and Radio Electronics, Siberian Federal University, Krasnoyarsk, Russian Federation
[e] Kirensky Institute of Physics FRC KSC SB RAS, FSBSI "Federal Research Center "Krasnoyarsk Science Center SB RAS", Krasnoyarsk, Russian Federation
[f] Tomsk State University, 634050, Tomsk, Russian Federation
[g] Emanuel Institute of Biochemical Physics, Russian Academy of Sciences, Moscow, 119334, Russian Federation
[h] Institute of Chemistry and Chemical Technology, FRC KSC SB RAS, FSBSI "Federal Research Center "Krasnoyarsk Science Center SB RAS", Krasnoyarsk, Russian Federation

ARTICLE INFO

Article history:
Received 9 November 2021
Received in revised form
6 December 2021
Accepted 6 December 2021
Available online 8 December 2021

Keywords:
Endohedral metallofullerenes
Fullerite
Pressure induced phase transformation
Density functional theory
Density functional based tight binding

ABSTRACT

In this work, through the technology of producing endohedral metallofullerene in macroscopic quantities, the process of pressure polymerization of $Sc_2C_2@C_{82}$ and their mechanical properties have been investigated in detail using a set of experimental and theoretical methods. The crucial role of endohedral atoms is demonstrated by comparison with pristine fullerenes. It is shown that the embedding of Sc_2C_2 complex inside a fullerene significantly facilitates the polymerization process which finally leads to the highly rigid material at high pressures.

1. Introduction

Even though fullerenes have been discovered more than 30 years ago [1] they still contain a lot of challenges for fundamental science. Studies of physicochemical, electrophysical and optical properties of fullerites under the high compressive pressures are still of significant interest for both experiment and theory. It is known that under the high pressure and high-temperature conditions, buckminsterfullerene C_{60} undergoes a series of phase transitions and transform into the polymer whose final structure depends on the exact processing conditions [2–4] which extends the carbon phase diagram by onion-like structures [5]. The polymers obtained from fullerenes are of considerable interest due to their wide range of applications (from solar cells [6] to ultra-hard materials [7–9]). At the same time, polymerization itself is a complex process whose description at the atomic level is a challenging task. A large number of fullerene isomers [10], the possibility of variable surface functionalization as well as the implantation of different atoms inside fullerenes, lead to a great variety of possible structures.

Indeed, shortly after the discovery of the buckminsterfullerene in the work [11], it has been shown that a cavity within the carbon frame of fullerene molecules can accommodate a variety of atoms, both non-metals (He, N, P) and metals, especially from a series of rare earth, with the formation of endohedral metallofullerene

* Corresponding author. National University of Science and Technology MISiS, 119049, Leninskiy prospect 4, Moscow, Russian Federation.
** Corresponding author. Technological Institute for Superhard and Novel Carbon Materials, 7a Tsentralnaya Street, Troitsk, Moscow, Russian Federation.
*** Corresponding author. Institute of Engineering Physics and Radio Electronics, Siberian Federal University, Krasnoyarsk, Russian Federation.
E-mail addresses: mikhail.popov@tisnum.ru (M.Yu. Popov), pbsorokin@tisnum.ru (P.B. Sorokin), alex99@iph.krasn.ru (A.S. Fedorov).

https://doi.org/10.1016/j.carbon.2021.12.040
0008-6223/

(EMF) molecules. Endohedral fullerenes belong to a new class of compounds which are technologically and scientifically important owing to their unique structures and optoelectronic properties [12]. In most endohedral metallofullerenes, the introduction of metal atoms into carbon cages leads to a change of the electron affinity relative to the corresponding empty cages [13]. Due to the low ionization potential of metal atoms, in most cases, from them to the carbon frame of the EMF 2–3 *e* are transferred. This leads to the emergence of many new properties that are not inherent to pristine structures making EMFs a potential candidate for photovoltaic and optical devices, elements of nanoelectronics and optoelectronics, biomedical engineering as high-performance contrast agents, etc. [12].

The transfer of electrons leads to a reduction of the HOMO-LUMO gap in the EMF and an increase in their chemical activity. This activity should potentially lead to easier polymerization of EMF-based fullerites at high temperatures and pressures compared to the case of C_{60} or other fullerites. Polymerized EMF can be a new material with promising applications in a wide range of scientific and technological fields. However, despite the promise, the extreme rarity of EMF makes it impossible to carry out a systematic large-scale study.

Because we have developed the technology to produce EMF in macroscopic quantities [14], for the first time we have been able to study the structural behavior of the Sc contained fullerenes under extreme conditions. In this study, using diamond anvil technology, we demonstrate how the endohedral metallofullerenes $Sc_2C_2@C_{82}$ can undergo polymerization under high pressure. The behavior of the EMF under the study was compared with empty caged fullerite which allowed to proceed the differences in the processes of polymerization of both types of fullerites. The experimental results were comprehended by density functional and density functional tight binding theories in which key features of the polymerization process were studied in detail. Finally, the mechanical properties of the polymerized material were investigated.

2. Materials and methods

Carbon condensate containing $Sc_2C_2@C_{82}$ was synthesized in a high-frequency arc discharge plasma by sputtering graphite electrodes with axial holes of 3 mm in diameter containing a mixture of Sc_2O_3 powder and graphite in a 1:1 mass ratio [14,15]. A mixture of fullerenes was extracted from the obtained carbon condensate using carbon disulfide in a Soxhlet apparatus. A mixture of $Sc_2C_2@C_{82}$ and higher fullerenes was obtained using Lewis acids $TiCl_4$ [16]. Fullerenes $Sc_2C_2@C_{82}$ and C_{84} were isolated from solution by high-performance liquid chromatography using an Agilent Technologies 1200 Series chromatograph (CosmosilBuckyprep M column, toluene flow 1.6 ml/min). To obtain mass spectra of fullerenes, a MALDI-TOF Bruker BIFLEX TM III mass spectrometer was used. X-ray photoelectron spectroscopy (XPS) studies were performed on a UNI-SPECS Spectrometer, SPECS Gmbh.

We used a shear diamond anvil cell (SDAC) for our high-pressure study. This procedure was used for activation of a possible phase transition by the application of shear deformation to the sample [17].

In the SDAC, controlled shear deformation was applied to the compressed sample by a rotation of one of the anvils around the anvil's symmetry axis [5]. The pressure was measured from the stress-induced shifts of the Raman spectra from the diamond anvil tip [18]. The Raman spectra were recorded with a Renishaw inVia Raman microscope (excitation wavelength 532 and 405 nm).

Besides experimental research, theoretical DFT calculations were performed within the generalized gradient approximation in the Perdew–Burke–Ernzerhof (GGA-PBE) parameterization. A periodic structure including 4 $Sc_2C_2@C_{82}$ molecules in the unit cell was investigated. We used the projector augmented wave (PAW) method [19] approximation with periodic boundary conditions implemented in Vienna Ab-initio Simulation Package (VASP) [20–23]. Plane-wave energy cut-off was equal to 550 eV. A structural relaxation was performed until forces acting on each atom became less than 10^{-2} eV/Å. Non-local van der Waals functional was used for correct describing intermolecular interactions as implemented in the vdW-DF1 method [24].

The relative stability of the polymerized phases of fullerite at finite pressure and temperature can be qualitatively determined by a simple compression with the calculation of their Gibbs free energies, $G = E + PV - TS$. The phonon spectra and phonon contributions to the entropy S were calculated by the frozen phonon method using DFTB+ package [25]. As a result, we were convinced that the change in the specific contribution of the phonon contribution of the entropy TS into the Gibbs free energy *G* with a change in the structure per atom is significantly less than the change in the total energy per atom when forming new C-C bonds during polymerization; therefore, in what follows, the contribution of TS to the free energy was not considered. So, our DFT calculations were performed at zero temperature and the Gibbs free energy was replaced by the enthalpy $H = E + PV$.

Additionally, a set of subsequent molecular dynamic (MD) simulations were performed within the framework of NCC-DFTB (non-consistent charge version of density functional-based tight binding) method [26,27] using DFTB+ package, standard *trans3d* [28] and compatible *mio* [29] parameter sets. MD simulations allow modeling the process of scandium EMF structural transformation under the external pressure emulating SDAC conditions.

Though the actual polymerization takes place at room temperature, it can't be explicitly modeled via MD simulations due to the limits of computational resources. This may be overcome by increasing the temperature of the system. This, in turn, accelerates the structural transformation providing a qualitative understanding of the main polymerization features. First, the optimized $Sc_2C_2@C_{82}$ unit cell taken from DFT calculations described above was heated up to 3000 K without any external pressure using the following temperature profile: 100 fs thermalization at 298 K, then heating from 298 to 3000 K within 5 ps and 10 ps structural evolution at 3000 K. Next, the pressure was increased stepwise from 5 to 30 GPa. For the sake of comparison, the same procedure was applied to the identical C_{82} unit cell without Sc_2C_2 dimers inside the fullerene cage.

3. Results and discussions

We have synthesized, extracted, and isolated $Sc_2C_2@C_{82}$ and C_{84}. The mass spectra of the chromatographic fractions are shown in Fig. 1. The molecular weights 1098 *m*/*z* (Fig. 1a) and 1008 *m*/*z* (Fig. 1b) as well as isotopic distribution of this peaks correspond to $Sc_2C_2@C_{82}$ and C_{84}, respectively. In Fig. 1a, molecular weights 1080, 1104, and 1128 *m*/*z* conform to C_{90}, C_{92}, and C_{94}, respectively whereas 1032 *m*/*z* (Fig. 1b) corresponds to C_{86}.

XPS was used to analyze samples of chromatographic fractions containing $Sc_2C_2@C_{82}$ and C_{84} before and after pressure treatment in the SDAC. The analysis results for sample C_{84} are shown in Fig. 2a. In the sample, after the pressure treatment, two peaks appeared corresponded to C–C sp^2- (284.8 eV), and sp^3-hybridized bonds (285.5 eV). The estimation of the quantity of the latter bonds yields the value of 23.9% whereas in the initial sample only sp^2-hybridized bonds were observed.

The XPS spectrum of Sc contained fullerite is more complex and contained peaks corresponded not only to C–C but also to O–C=O bonding (Fig. 2b). The distribution of the binding energy of the C1s

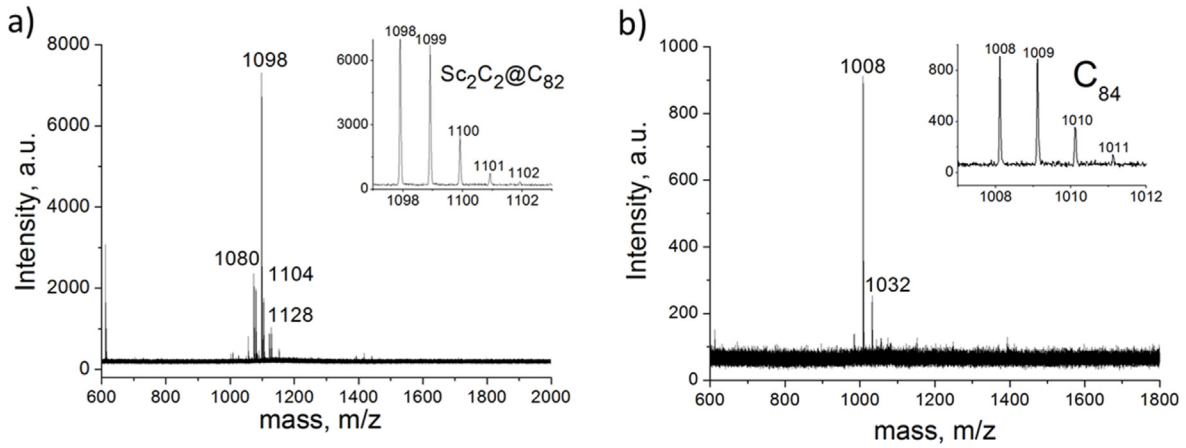

Fig. 1. Mass spectrum (+) of chromatographic fraction of extracted fullerites. a) $Sc_2C_2@C_{82}$ and b) C_{84}.

line in the initial sample of EMF before pressure treatment made it possible to determine the degree of carbon sp^2- (58.43% of the area of the C 1s line) and sp^3-hybridization (11.56%). Also, we estimated the degree of O–C=O bonds as 10.36% (288.5 eV) and Si–C bonds as 19.65% (283.2 eV). The latter signal was probably originated from the non-volatile micropowder. We can speculate that due to the very small sample volume and the small diameter of the focusing spot, the micropowder was trapped in the spot area during several measurements. The Si–C line disappears after etching with Ar^+ ions, which confirms this surface contamination, but the fullerene also begins to decompose, and this leads to the transformation of the entire spectrum. After pressure treatment, the contamination disappeared and the final degree of sp^3-hybridization reached 30.19%, while the degree of sp^2-hybridized bonds was 57.98%, and O–C=O was 11.84%.

Decomposition of the Sc 2p line showed the presence of Sc^{2+} according to the literature [30]. It should be mentioned that in 2006 the assignment of the main isomer Sc_2C_{84} to $Sc_2C_2@C_{82}$ was carried out using NMR spectroscopy [31]. Later, this fact was confirmed by powder synchrotron X-ray diffraction with Rietveld analysis [32]. Analysis showed that the Sc 2p line remained unchanged after pressure (Fig. 2c). Thus, it was shown that in $Sc_2C_2@C_{82}$ after treatment with quasistatic pressure, the proportion of carbon with sp^3-hybridization increased, while the Sc^{2+} line did not change.

According to the results of the experimental synthesis where $Sc_2C_2@C_{82}$ were obtained we designed the corresponding model which can form chemically connected atoms in the periodical supercell and does not require considering a large number of atoms. The last is especially important because it allows us to carry out a thorough analysis via DFT and DFTB calculations. Although in the experiment the behavior of $Sc_2C_2@C_{82}$ under the pressure was compared with pure C_{84} fullerenes behavior, in the calculations a comparison of C_{82} with and without guest atoms was carried out to obtain clarity about the role of the Sc_2C_2 complex. A large number of isomers for fullerenes larger than buckminsterfullerene C_{60} allows us to assume that the experimental samples can contain various isomers. Under this assumption, we have designed the model consisting of three isomers C_{82} C_{2v} which have the lowest shell curvature energy, and one C_{82} C_{3v} with the symmetry allowed to construct a dense polymerized cell. We found that C_{82} C_{3v} and C_{2v} isomers bond with each other with the formation of a dense polymer with maximal a sp^3-bonding fraction of 65% (Fig. 3a). The bonds between fullerenes in a polymer are differ depending on the type of isomer. Each fullerene is surrounded by $12C_{82}$. C_{2v} isomer bonds with 11 fullerenes by cycloaddition reaction type (3 + 3), (4 + 4), and (2 + 2) (see Fig. 3b) whereas C_{3v} isomer connects with 9 surrounded fullerenes by (2 + 2) and (3 + 3) bonding. The C_{3v} isomer bonding with other fullerenes only threw hexagon rings and did not involve 5-membered rings, in contrast to the C_{2v} isomers. The other 3 C_{2v} fullerenes are connected differently. One of them forms 2 bonds with C_{3v} fullerene by (5 + 4) cycloaddition reaction type (see Fig. 3b), the second forms only one bond and the third is not connected.

In the next step, we determined the positions of the guest groups Sc_2C_2 inside the C_{82} molecule. Due to the complexity of the potential hypersurface of Sc_2C_2 inside a fullerene, we performed a multi-step search for its favorable position. First, initial relaxation of the structures was performed by using simulated annealing based on *ab initio* molecular dynamics, to evaluate a large number of starting structures. For each simulation, the temperature was increased rapidly up to 1500 K and lowered gradually to 1 K, with a time step of 0.5 fs during 1 ps (Fig. 3c). The resulting C_{3v} and C_{2v} $Sc_2C_2@C_{82}$ structures obtained by molecular dynamics were finally relaxed. It was obtained that the Sc_2C_2 molecule behaves similarly in both isomers. The scandium atoms always tend to fix above the hexagonal rings on opposite sides while the C_2 molecule is located in the cavity center with a typical bond length of 1.27 Å.

The polymerization of fullerenes can be represented as a phase transformation from an unbound molecular form to a chemically bonded polymerized state. It is convenient to consider this process through the enthalpy H dependences of the corresponding phases on the pressure. They were obtained by structural optimization of molecular and polymerized fullerites with a gradual increase of the isotropically applied external pressure. It is obtained that both C_{82} and $Sc_2C_2@C_{82}$ are not able to reach maximal polymerization but their behavior under the pressure has a fundamentally different character.

Thus, in the case of pristine fullerenes, we found that the enthalpies of fully polymerized structure and molecular fullerite (red line in Fig. 4a) intersect at 23 GPa which allows us to propose the stepwise increase in sp^3-hybridized bonds at this pressure. Before that, at 15 GPa, only rare sp^3 bonds begin to form in the molecular phase (Fig. 4a, inset). With further increase in pressure the percentage of these bonds increases, however, it does not exceed 6% until 23 GPa. The minimization algorithm of DFT does not allow spontaneous transformation from partial to full polymerization at 23 GPa and, thus, it is possible to study the intermolecular bonding in the partially polymerized state also at higher pressures.

In the case of the EMF, we got a completely different behavior of the structure under pressure. It is obtained that pressure

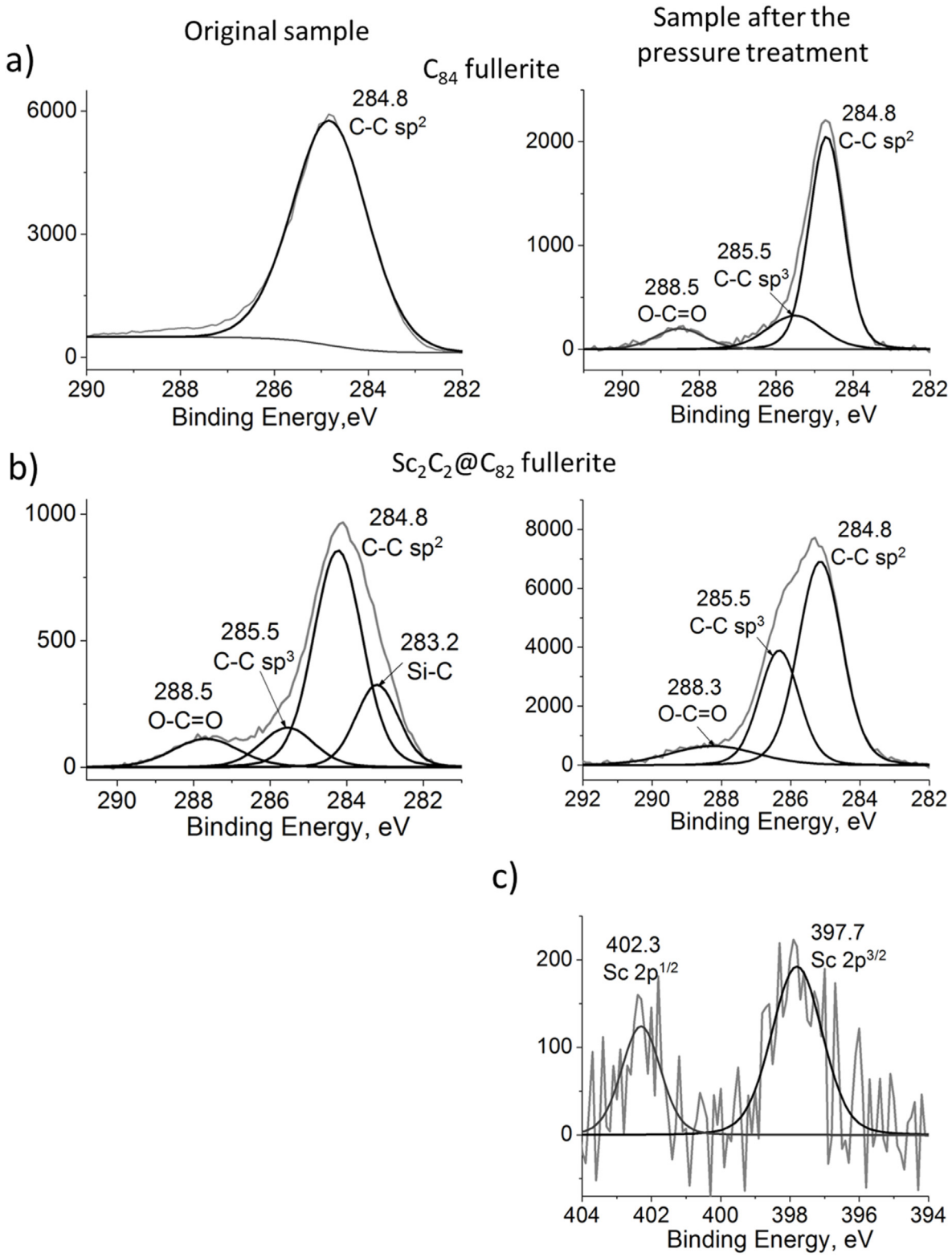

Fig. 2. X-ray photoelectron spectroscopy analysis of fullerite sample before and after the pressure treatment. XPS of C1s line of a) C_{84} and b) $Sc_2C_2@C_{82}$ before (left) and after pressure treatment (right); c) XPS of $Sc_2C_2@C_{82}$ Sc^{2+} after the pressure treatment.

application leads to a gradual increase of sp^3 bonds in the structure without the appearance of a phase transition into a fully polymerized structure, which is clear from the asymptotic behavior of the enthalpy difference with pressure increasing (blue line in Fig. 4b). The increasing of pressure leads to a smooth incremental formation of the polymerized structure from 12.5 GPa with a sp^3-hybridization degree increasing until 23% at 27.5 GPa (Fig. 4b, inset). This result allows us to conclude that Sc encapsulation

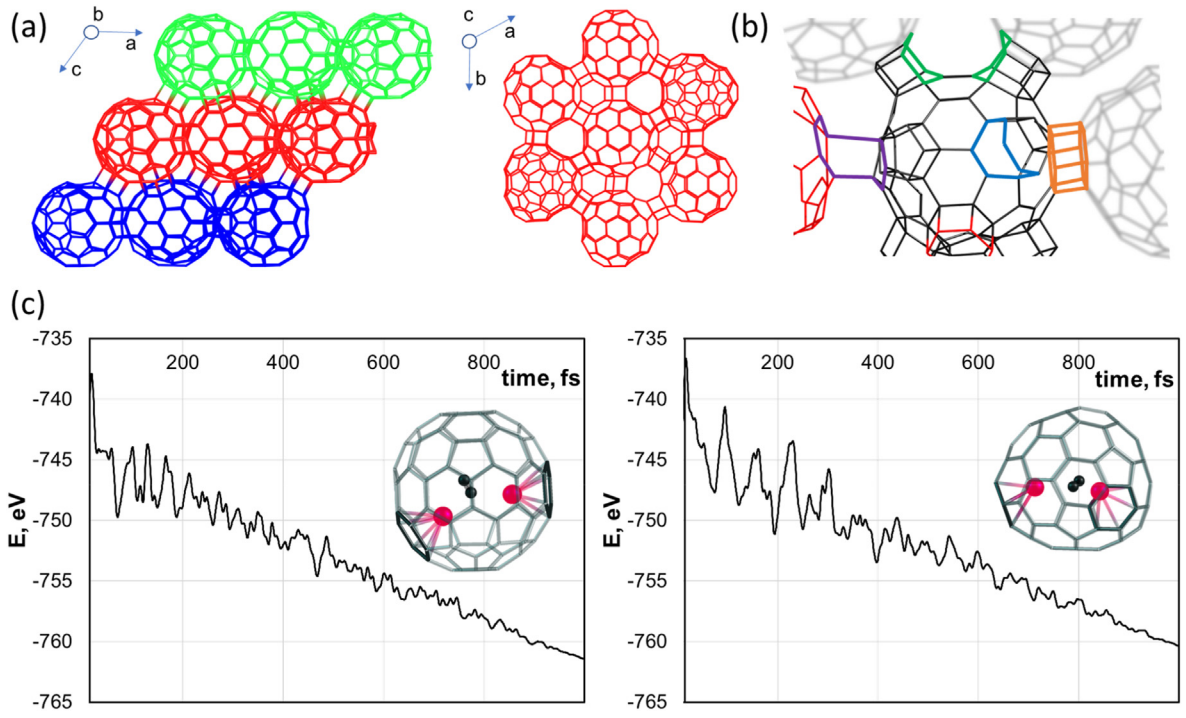

Fig. 3. Determination of the atomic structure. a) Cross-section view of fully polymerized fullerite C_{82} (left) and its single layer (right); b) Connection type between C_{2v} (black) and C_{3v} (red) isomers of fullerene. The cycloaddition (3 + 3), (4 + 4), (2 + 2), and (5 + 4) are marked by green, blue, orange and violet respectively. The final relaxed structure of the C_{82} and $Sc_2C_2@C_{82}$ polymer contains sp^3 bonds fraction of 65% and 50%, respectively; c) potential energy and structural changes of $Sc_2C_2@C_{82}$ isomers C_{2v} (left) and C_{3v} (right) in simulations annealing. The insets show the final structures of both isomers with bolded hexagon rings connected with the Sc atoms. In all geometries, the carbon bonds are marked with thin sticks while the inner C and Sc atoms are gray and pink balls, respectively. (A colour version of this figure can be viewed online.)

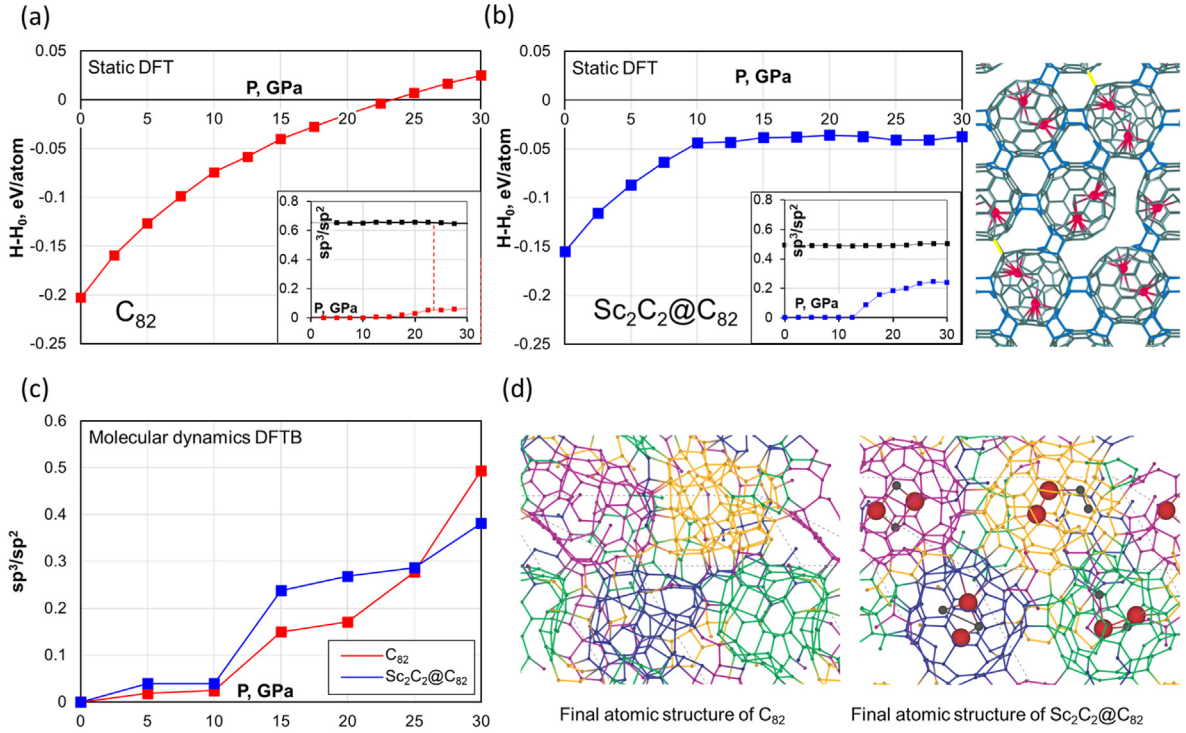

Fig. 4. Fullerenes C_{82} and $Sc_2C_2@C_{82}$ polymerization process description. a,b) Difference between enthalpies H of initially molecular (red and blue lines) and fully polymerized fullerene H_0 for C_{82} (a) and $Sc_2C_2@C_{82}$ (b) vs. pressure. In the insets, the dependence of relation between the amount of sp^3- and sp^2-hybridized bonds of both initially molecular (red and blue lines) and fully polymerized fullerene (black line) on the pressure are presented. In (b) the atomic structure of polymerized $Sc_2C_2@C_{82}$ at pressure 27.5 GPa is also presented. The cycloaddition (4 + 4) is marked by blue. The single bonding is marked by yellow; c) process of C_{82} (red line) and $Sc_2C_2@C_{82}$ (blue line) fullerenes polymerization during pressure increasing up to 30 GPa simulated in the framework of DFTB. d) Final geometries of fullerenes C_{82} and EMF $Sc_2C_2@C_{82}$ at 30 GPa. Different colors correspond to atoms of different fullerene cages. In all geometries, the carbon bonds are marked with thin sticks while the inner C and Sc atoms are gray and pink balls, respectively. (A colour version of this figure can be viewed online.)

smooth and relieve the polymerization process. The Bader charge analysis shows that in molecular $Sc_2C_2@C_{82}$ each scandium gives 1.54*e* in total, 1.21*e* is taken by the inner C_2 (0.48*e* and 0.73*e*), and the remaining 1.87 electrons transfer to fullerene framework, causing its slight polarization, the region near the scandium is more negatively charged compared to the remaining fullerene atoms. In the case of polymer formation, the polarization becomes slightly less, the charge on Sc_2 decreases by 0.2*e* (1.45*e* per scandium) with transferring of 1.66*e* to fullerene framework. This allows us to conclude that the presence of scandium inside the fullerene polarizes the carbon bonds, which leads to an increase in their chemical activity and facilitates polymerization. The presence of scandium within the fullerene makes the (4 + 4) cycloaddition reaction more uniform. Almost all fullerenes bind through (4 + 4) bonds, although individual ones are also present (Fig. 4b). Unlike pristine fullerite, not all fullerenes bond with each other.

The polymerization process of the pristine fullerenes C_{82} or in EMF $Sc_2C_2@C_{82}$ was theoretically investigated by DFTB MD calculations. The use of the semiempirical approach allows long term molecular dynamic simulation, however, since this approach is less accurate, only a qualitative agreement with DFT and experiment can be expected. Within this approximation, dynamic polymerization was traced with a gradual increase of pressure up to 30 GPa at fixed temperature T = 3000 K. As in the above, we observed rising the number of sp^3 bonds with increasing pressure (the chemical bonds of inner Sc_2C_2 group and fullerene cage was not taken into account), see Fig. 4c. In agreement with DFT calculations, in the EMF case, polymerization up to a pressure of 25 GPa proceeds faster, then the number of sp^3 bonds between pristine fullerenes increases and overlaps the corresponding value for EMF at 30 GPa. The final structures are significantly deformed, but the carbon framework is preserved, which suggests the successful completion of the polymerization process in both considered cases (Fig. 4d).

The predicted behavior was studied in the experiment. The $Sc_2C_2@C_{82}$ samples are strongly luminescent. The Raman spectra (Fig. 5a) lack the narrow modes characteristic of fullerenes in the region of breathing, intermediate and tangential frequencies usually observed, in particular, for higher fullerenes [13,33]. Nevertheless, a 1436 cm^{-1} mode is present on the spectra which is assigned to the pentagonal-pinch mode (involved tangential displacements of carbon atoms with pressing pentagons and widening adjacent hexagons) [1]. This mode is centered at 1469 cm^{-1} in the Raman spectra of the fullerene C_{60} [1]. The position of the maximum of the pentagonal-pinch mode depends on a curvature of the fullerene-type onion shell and a particular arrangement of surrounding hexagons [1,34]. The spectra also show broad bands around 1273, 1363, and 1602 cm^{-1}, the appearance of these bands can be explained by the broadening of the $Sc_2C_2@C_{82}$ lines. The reason for this smearing and broadening of the lines is not clear, since the metal encapsulated fullerenes retain distinguishable peaks corresponding to phonon modes [13,33].

With increasing pressure (up to 20 GPa), no noticeable changes were observed in the Raman spectra of the sample (Fig. 5b). At a pressure of 20 GPa, shear strains were applied to the sample (anvil rotation angle was 12°). Fig. 5c shows the dependence of the most intense line (1602 cm^{-1} on the original sample) on pressure. Values related to the sample before shear strain application are marked by circles, and after shear strain application (pressure decrease) are marked by crosses.

It can be seen from Fig. 5c that at pressures ~2 GPa, 7 GPa, and 17 GPa the beginning of so-called softening of Raman modes is observed (pressure increase leads to sharp deceleration of frequency growth with its subsequent decrease). This result correlates well with the theoretical prediction of a gradually increasing degree of polymerization with pressure. Earlier such phenomenon was observed for C_{60}, and at the same values of pressures [35]. However, in contrast to C_{60}, at pressures below ~5 GPa the reverse transition to the initial state occurred (Fig. 5c), which is also very well correspond with the theory where gradually polymerization of EMF without phase transition means possible reverse transformation. Raman spectra of the original sample and the sample treated with 20 GPa pressure and shear deformation do not differ (Fig. 5a).

When the sample is unloaded in the pressure range from 20 to 6 GPa the dependence of Raman frequency on pressure is linear. This makes it possible to estimate the bulk modulus of the high-pressure phase B_0 = 509 GPa according to the approach given in Refs. [36,37] An indirect confirmation of the B_0 value (exceeding the bulk modulus of the diamond 443 GPa) is the fact that the diamond anvil is scraped by the sample while rotating (Fig. 5d) [35]. According to the definition of the ultrahigh hardness introduced in Ref. [38], trenching is only possible when the hardness (which is numerically related to the yield strength) of the $Sc_2C_2@C_{82}$ sample exceeds the hardness (and therefore the yield strength) of the diamond. Ref. [39] shows that the yield strength (and plasticity mechanisms) of covalently bonded materials at temperatures below the Debye temperature are determined mostly by their elastic moduli. Therefore, the high bulk modulus measured in the work and exceeding the bulk modulus of diamond confirms the observed ultrahigh hardness of the sample $Sc_2C_2@C_{82}$ at pressures from 20 to 6 GPa.

For comparison, the SDAC study of C_{84} samples was carried out. Samples C_{84} luminesce are significantly stronger than $Sc_2C_2@C_{82}$. As a result, the Raman spectra observed only a peak of 1602 cm^{-1} (Fig. 6a). The Raman spectrum of the original sample and after treatment with a pressure of 25 GPa with a shift did not change. The absence of the D mode indicates that this is not soot (i.e., not disordered graphene-like layers). Raman spectra of sample C_{84} under pressure are shown in Fig. 6b.

The dependence of Raman frequency on pressure (Fig. 6c) shows 3 phase transitions with increasing pressure: at pressures ~2 GPa, ~10 GPa, and ~17 GPa. At a pressure of 25 GPa shear strains were applied (anvil rotation at an angle of 12°). No phase transitions were observed during unloading.

Similarly, to the $Sc_2C_2@C_{82}$ sample, the bulk modulus B_0 = 330 GPa of the high-pressure phase C_{84} was estimated from the Raman frequency dependence of the pressure. In contrast to the $Sc_2C_2@C_{82}$ sample, the diamond anvils in this experiment remained undamaged, which directly indicates a lower hardness than that of diamond and which is also indirectly indicated by the lower bulk modulus of compression of the sample. This can be related to lower fraction of sp^3 bonds in the sample in comparison with EMF and it correlates well with theoretical predictions of lower polymerization of C_{82} structure.

4. Conclusions

The presented work is the first study of the properties of the fullerite scandium endohedral complex as a bulk material. The process of fullerene polymerization was studied, and the governing role of embedded scandium atoms was demonstrated. It was shown experimentally that guest atoms facilitated the polymerization process. DFT and DFTB simulations demonstrated that scandium atoms change the fullerene bonding process completely by the polarization of the carbon bonds, which leads to an increase in their chemical activity. The mechanical properties of the resulting polymerized material were investigated, and its highest bulk modulus and hardness were observed. The authors hope that this work will pave the way for studies of fullerite endohedral complexes as a macroscopic material. This will make it possible to

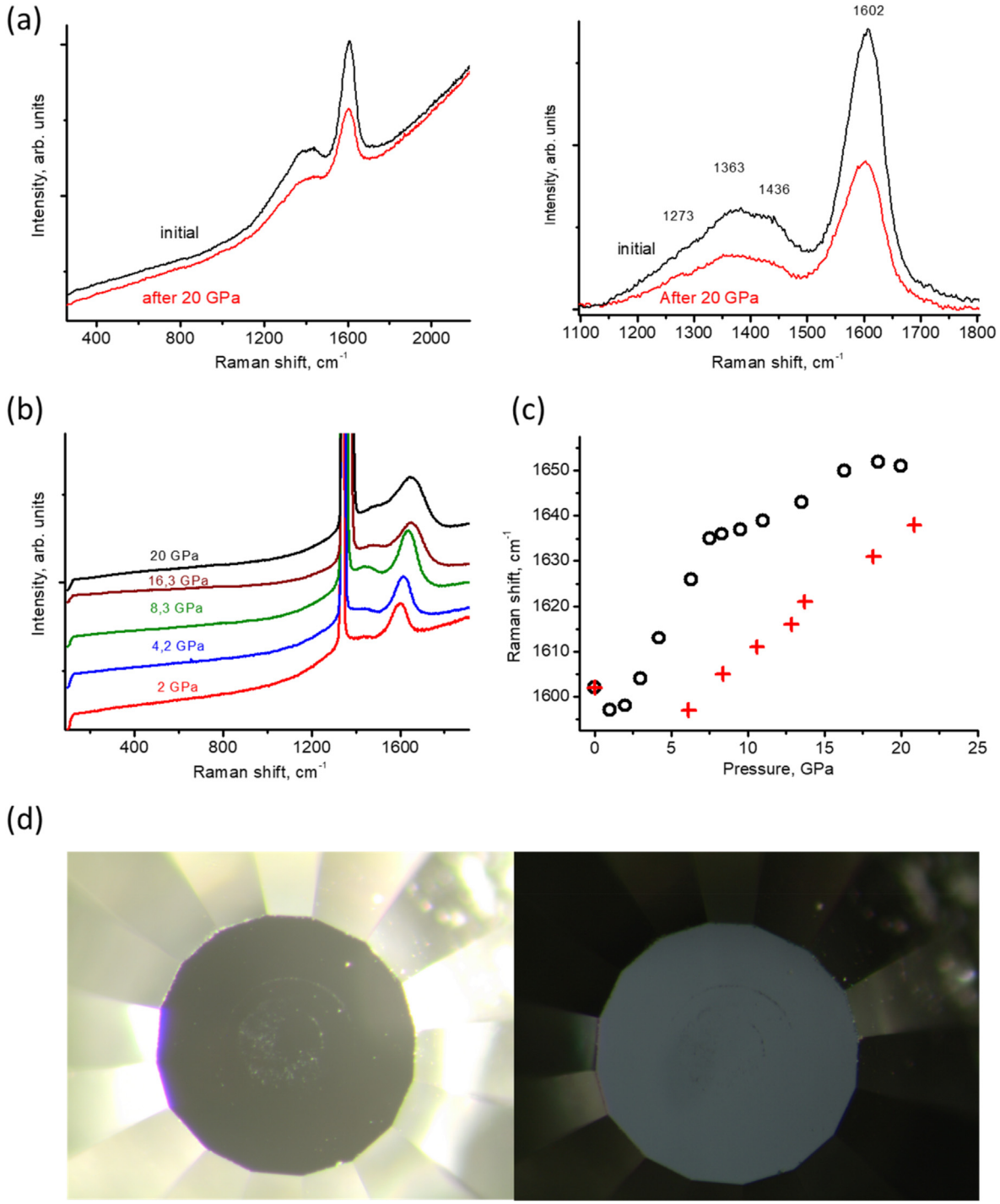

Fig. 5. The behavior of $Sc_2C_2@C_{82}$ under the pressure. a) Raman spectrum of the original sample and after treatment with 20 GPa shear pressure without (left) and after (right) baseline subtraction. Excitation frequency 405 nm; b) Raman spectrum change of the sample under pressure; c) Dependence of the most intense line (1602 cm^{-1} on the original sample) from the pressure. Values referring to the sample before shear strain application are indicated by circles, and after shear strain application (pressure decrease) are indicated by crosses. d) Grooves on the surface of the diamond anvil resulting from trenching of the $Sc_2C_2@C_{82}$ sample at a shear pressure of 20 GPa. The diameter of the anvil is 0.4 mm. (A colour version of this figure can be viewed online.)

consider EMF not only as a nanostructure of only fundamental interest but also as a promising material that may be in demand in various fields of science and technology in the future.

CRediT authorship contribution statement

S.V. Erohin: Methodology, Software, Investigation. **V.D. Churkin:** Formal analysis, Investigation, Visualization. **N.G. Vnukova:** Formal analysis, Investigation. **M.A. Visotin:** Investigation, Visualization. **E.A. Kovaleva:** Software. **V.V. Zhukov:** Software, Investigation. **L.Yu. Antipina:** Formal analysis, Writing – original draft, Visualization. **Ye.V. Tomashevich:** Formal analysis. **Yu.L. Mikhlin:** Formal analysis. **M.Yu. Popov:** Writing – original draft, Supervision. **G.N. Churilov:** Supervision. **P.B. Sorokin:**

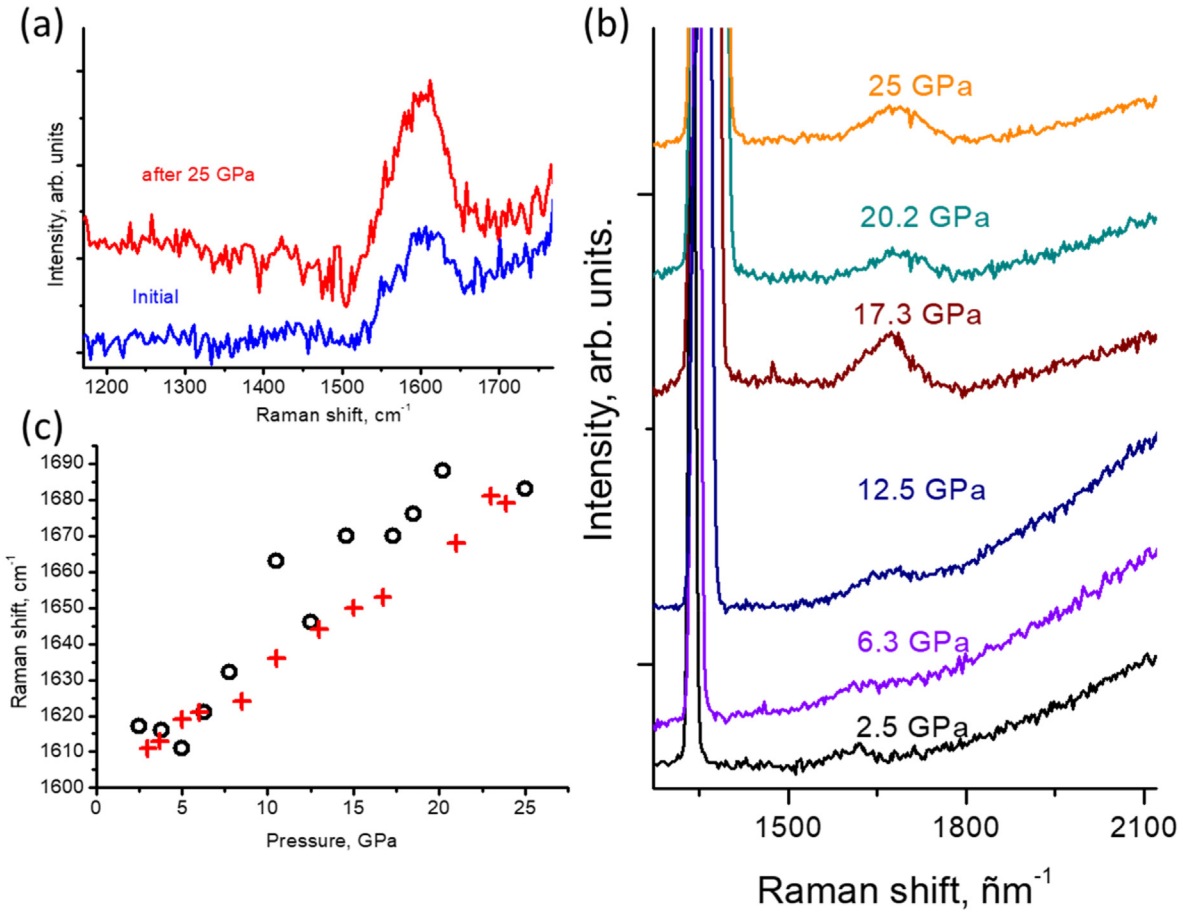

Fig. 6. Measured behavior of C_{84} under the pressure. a) Raman spectrum of the original sample and after treatment with 25 GPa pressure with a shift after baseline subtraction. The excitation frequency is 405 nm. Only the peak of 1602 cm^{-1} is visible against the strong luminescence in the background; b) Raman spectrum of sample under pressure; c) Dependence of the most intense line (1602 cm^{-1} on the original sample) from the pressure. Values referring to the sample before shear strain application are indicated by circles, and after shear strain application (pressure decrease) are indicated by crosses. (A colour version of this figure can be viewed online.)

Conceptualization, Writing – original draft, Writing – review & editing, Visualization, Supervision. **A.S. Fedorov:** Conceptualization, Supervision, Funding acquisition.

Declaration of competing interest

The authors declare that they have no known competing financial interests or personal relationships that could have appeared to influence the work reported in this paper.

Acknowledgements

The authors gratefully acknowledge the financial support of RFBR (Project identifier:18-29-19080). The calculations were performed at supercomputer cluster provided by the Materials Modeling and Development Laboratory at NUST “MISIS” and Joint Supercomputer Center of the Russian Academy of Sciences. The authors thank the staff of the Information Technology Department of the Moscow Institute of Physics and Technology and express their gratitude to the Data Center Group for their help in making calculations. M.P. acknowledges the support of the Ministry of Science and Higher Education of the Russian Federation in the framework of the State Task (project code 0718-2020-0037) for Raman study, interpretation, and discussion of obtained results as well as Russian Science Foundation (project #20-12-00097) for investigation of fullerite mechanical properties. V.D.C. acknowledges the support of RFBR (Project identifier:20-32-90038).

References

[1] M.S. Dresselhaus, G. Dresselhaus, P.C. Eklund, Science of Fullerenes and Carbon Nanotubes, Academic Press, USA, 1996.
[2] V.D. Blank, S.G. Buga, G.A. Dubitsky, N.R. Serebryanaya, M.Y. Popov, B. Sundqvist, High-pressure polymerized phases of C60, Carbon 36 (1998) 319–343, https://doi.org/10.1016/S0008-6223(97)00234-0.
[3] N.R. Serebryanaya, V.D. Blank, V.A. Ivdenko, L.A. Chernozatonskii, Pressure-induced superhard phase of C60, Solid State Commun. 118 (2001) 183–187, https://doi.org/10.1016/S0038-1098(01)00082-5.
[4] L.A. Chernozatonskii, N.R. Serebryanaya, B.N. Mavrin, The superhard crystalline three-dimensional polymerized C60 phase, Chem. Phys. Lett. 316 (2000) 199–204.
[5] V.D. Blank, V.D. Churkin, B.A. Kulnitskiy, I.A. Perezhogin, A.N. Kirichenko, V.N. Denisov, S.V. Erohin, P.B. Sorokin, M.Y. Popov, Phase diagram of carbon and the factors limiting the quantity and size of natural diamonds, Nanotechnology 29 (2018) 115603, https://doi.org/10.1088/1361-6528/aaa857.
[6] S. Collavini, J.L. Delgado, Fullerenes: the stars of photovoltaics, Sustain. Energy Fuels 2 (2018) 2480–2493, https://doi.org/10.1039/C8SE00254A.
[7] V. Blank, S. Buga, G. Dubitsky, N. Serebryanaya, M. Popov, V. Prokhorov, Properties and applications of superhard and ultrahard fullerites, in: Eiji Osawa (Ed.), Perspect. Fuller. Nanotechnol., Kluwer Academic Press, Dordrecht, 2002, pp. 223–233.
[8] L. Wang, B. Liu, H. Li, W. Yang, Y. Ding, S.V. Sinogeikin, Y. Meng, Z. Liu, X.C. Zeng, W.L. Mao, Long-range ordered carbon clusters: a crystalline material with amorphous building blocks, Science 337 (2012) 825–828.
[9] S. Zhang, Z. Li, K. Luo, J. He, Y. Gao, A.V. Soldatov, V. Benavides, K. Shi, A. Nie, B. Zhang, W. Hu, M. Ma, Y. Liu, B. Wen, G. Gao, B. Liu, Y. Zhang, Y. Shu, D. Yu, X.-F. Zhou, Z. Zhao, B. Xu, L. Su, G. Yang, O.P. Chernogorova, Y. Tian, Discovery of carbon-based strongest and hardest amorphous material, Natl. Sci. Rev.

(2021), https://doi.org/10.1093/nsr/nwab140.
[10] P.W. Fowler, D.E. Manolopoulos, An Atlas of Fullerenes, Oxford University Press, Oxford, 1995.
[11] J.R. Heath, S.C. O'Brien, Q. Zhang, Y. Liu, R.F. Curl, F.K. Tittel, R.E. Smalley, Lanthanum complexes of spheroidal carbon shells, J. Am. Chem. Soc. 107 (1985) 7779–7780, https://doi.org/10.1021/ja00311a102.
[12] A.A. Popov, S. Yang, L. Dunsch, Endohedral fullerenes, Chem. Rev. 113 (2013) 5989–6113, https://doi.org/10.1021/cr300297r.
[13] S. Guha, K. Nakamoto, Electronic structures and spectral properties of endohedral fullerenes, Coord. Chem. Rev. 249 (2005) 1111–1132, https://doi.org/10.1016/j.ccr.2004.11.017.
[14] G.N. Churilov, A.A. Popov, N.G. Vnukova, A.I. Dudnik, G.A. Glushchenko, N.A. Samoylova, et al., A method and apparatus for high-throughput controlled synthesis of fullerenes and endohedral metal fullerenes, Tech. Phys. Lett. 42 (2016) 475–477, https://doi.org/10.1134/S1063785016050072.
[15] G.N. Churilov, W. Krätschmer, I.V. Osipova, G.A. Glushenko, N.G. Vnukova, A.L. Kolonenko, A.I. Dudnik, Synthesis of fullerenes in a high-frequency arc plasma under elevated helium pressure, Carbon 62 (2013) 389–392, https://doi.org/10.1016/j.carbon.2013.06.022.
[16] K. Akiyama, T. Hamano, Y. Nakanishi, E. Takeuchi, S. Noda, Z. Wang, S. Kubuki, H. Shinohara, Non-HPLC rapid separation of metallofullerenes and empty cages with TiCl4 Lewis acid, J. Am. Chem. Soc. 134 (2012) 9762–9767, https://doi.org/10.1021/ja3030627.
[17] V. Blank, M. Popov, S. Buga, V. Davydov, V.N. Denisov, A.N. Ivlev, B.N. Marvin, V. Agafonov, R. Ceolin, H. Szwarc, A. Rassat, Is C60 fullerite harder than diamond? Phys. Lett. A 188 (1994) 281–286, https://doi.org/10.1016/0375-9601(94)90451-0.
[18] M. Popov, Pressure measurements from Raman spectra of stressed diamond anvils, J. Appl. Phys. 95 (2004) 5509–5514.
[19] P.E. Blöchl, Projector augmented-wave method, Phys. Rev. B 50 (1994) 17953–17979, https://doi.org/10.1103/PhysRevB.50.17953.
[20] G. Kresse, J. Furthmüller, Efficiency of ab-initio total energy calculations for metals and semiconductors using a plane-wave basis set, Comput. Mater. Sci. 6 (1996) 15–50, https://doi.org/10.1016/0927-0256(96)00008-0.
[21] G. Kresse, J. Furthmüller, Efficient iterative schemes for ab initio total-energy calculations using a plane-wave basis set, Phys. Rev. B 54 (1996) 11169–11186, https://doi.org/10.1103/PhysRevB.54.11169.
[22] G. Kresse, J. Hafner, Ab initio molecular dynamics for liquid metals, Phys. Rev. B 47 (1993) 558–561, https://doi.org/10.1103/PhysRevB.47.558.
[23] G. Kresse, J. Hafner, Ab initio molecular-dynamics simulation of the liquid-metal–amorphous-semiconductor transition in germanium, Phys. Rev. B 49 (1994) 14251–14269, https://doi.org/10.1103/PhysRevB.49.14251.
[24] M. Dion, H. Rydberg, E. Schröder, D.C. Langreth, B.I. Lundqvist, Van der Waals density functional for general geometries, Phys. Rev. Lett. 92 (2004) 246401, https://doi.org/10.1103/PhysRevLett.92.246401.
[25] B. Hourahine, B. Aradi, V. Blum, F. Bonafé, A. Buccheri, C. Camacho, C. Cevallos, M.Y. Deshaye, T. Dumitrică, A. Dominguez, S. Ehlert, M. Elstner, T. van der Heide, J. Hermann, S. Irle, J.J. Kranz, C. Köhler, T. Kowalczyk, T. Kubař, I.S. Lee, V. Lutsker, R.J. Maurer, S.K. Min, I. Mitchell, C. Negre, T.A. Niehaus, A.M.N. Niklasson, A.J. Page, A. Pecchia, G. Penazzi, M.P. Persson, J. Řezáč, C.G. Sánchez, M. Sternberg, M. Stöhr, F. Stuckenberg, A. Tkatchenko, V.W. -z. Yu, T. Frauenheim, DFTB+, a software package for efficient approximate density functional theory based atomistic simulations, J. Chem. Phys. 152 (2020) 124101, https://doi.org/10.1063/1.5143190.
[26] D. Porezag, Th. Frauenheim, Th. Köhler, G. Seifert, R. Kaschner, Construction of tight-binding-like potentials on the basis of density-functional theory: application to carbon, Phys. Rev. B 51 (1995) 12947–12957, https://doi.org/10.1103/PhysRevB.51.12947.
[27] T. Frauenheim, G. Seifert, M. Elstner, T. Niehaus, C. Köhler, M. Amkreutz, M. Sternberg, Z. Hajnal, A.D. Carlo, S. Suhai, Atomistic simulations of complex materials: ground-state and excited-state properties, J. Phys. Condens. Matter 14 (2002) 3015–3047, https://doi.org/10.1088/0953-8984/14/11/313.
[28] G. Zheng, H.A. Witek, P. Bobadova-Parvanova, S. Irle, D.G. Musaev, R. Prabhakar, K. Morokuma, M. Lundberg, M. Elstner, C. Köhler, T. Frauenheim, Parameter calibration of transition-metal elements for the spin-polarized self-consistent-charge density-functional tight-binding (DFTB) method:Sc ,Ti ,Fe ,Co ,and Ni, J. Chem. Theor. Comput. 3 (2007) 1349–1367, https://doi.org/10.1021/ct600312f.
[29] M. Elstner, D. Porezag, G. Jungnickel, J. Elsner, M. Haugk, Th. Frauenheim, S. Suhai, G. Seifert, Self-consistent-charge density-functional tight-binding method for simulations of complex materials properties, Phys. Rev. B 58 (1998) 7260–7268, https://doi.org/10.1103/PhysRevB.58.7260.
[30] T. Takahashi, A. Ito, M. Inakuma, H. Shinohara, Divalent scandium atoms in the cage of C84, Phys. Rev. B 52 (1995) 13812–13814, https://doi.org/10.1103/PhysRevB.52.13812.
[31] Y. Iiduka, T. Wakahara, K. Nakajima, T. Tsuchiya, T. Nakahodo, Y. Maeda, T. Akasaka, N. Mizorogi, S. Nagase, 13C NMR spectroscopic study of scandium dimetallofullerene, Sc2@C84 vs. Sc2C2@C82, Chem. Commun. (2006) 2057–2059, https://doi.org/10.1039/b601738j.
[32] H. Kurihara, X. Lu, Y. Iiduka, H. Nikawa, M. Hachiya, N. Mizorogi, Z. Slanina, T. Tsuchiya, S. Nagase, T. Akasaka, X-ray structures of Sc2C2@C2n (n = 40–42): in-depth understanding of the core–shell interplay in carbide cluster metallofullerenes, Inorg. Chem. 51 (2012) 746–750, https://doi.org/10.1021/ic202438u.
[33] M. Krause, M. Hulman, H. Kuzmany, T.J.S. Dennis, M. Inakuma, H. Shinohara, Diatomic metal encapsulates in fullerene cages: a Raman and infrared analysis of C84 and Sc2@C84 with D2d symmetry, J. Chem. Phys. 111 (1999) 7976–7984, https://doi.org/10.1063/1.480131.
[34] D.C. Pujals, O.A. de Fuentes, L.F.D. García, E. Cazzanelli, L.S. Caputi, Raman spectroscopy of polyhedral carbon nano-onions, Appl. Phys. A 120 (2015) 1339–1345.
[35] M. Popov, V. Mordkovich, S. Perfilov, A. Kirichenko, B. Kulnitskiy, I. Perezhogin, V. Blank, Synthesis of ultrahard fullerite with a catalytic 3D polymerization reaction of C60, Carbon 76 (2014) 250–256, https://doi.org/10.1016/j.carbon.2014.04.075.
[36] M. Popov, M. Kyotani, Y. Koga, Superhard phase of single wall carbon nanotube: comparison with fullerite C60 and diamond, Diam. Relat. Mater. 12 (2003) 833–839.
[37] D.S. Lugvishchuk, E.B. Mitberg, B.A. Kulnitskiy, E.A. Skryleva, Y.N. Parkhomenko, M.Yu. Popov, V.D. Churkin, V.Z. Mordkovich, Irreversible high pressure phase transformation of onion-like carbon due to shell confinement, Diam. Relat. Mater. 107 (2020), https://doi.org/10.1016/j.diamond.2020.107908, 107908.
[38] V.D. Blank, S.G. Buga, N.R. Serebryanaya, V.N. Denisov, G.A. Dubitsky, A.N. Ivlev, B.N. Mavrin, M.Yu. Popov, Ultrahard and superhard carbon phases produced from C60 by heating at high pressure: structural and Raman studies, Phys. Lett. A 205 (1995) 208–216.
[39] J.J. Gilman, Chemistry and Physics of Mechanical Hardness, John Wiley & Sons, 2009.